

Correctness Learning: Deductive Verification Guided Learning for Human-AI Collaboration

Zhao Jin¹, Lu Jin¹, Yizhe Luo¹, Shuo Feng¹, Yucheng Shi¹, Kai Zheng², Xinde Yu^{*1} and Mingliang Xu^{*1}

¹Zhengzhou University

²University of Electronic Science and Technology

{jinzhao, luoyizhe, fengshuo, ieycshi, iexumingliang}@zzu.edu.cn, {j18790929616, yxdz2022}@163.com, zhengkai@uestc.edu.cn

Abstract

Despite significant progress in AI and decision-making technologies in safety-critical fields, challenges remain in verifying the correctness of decision output schemes and verification-result driven design. We propose correctness learning (CL) to enhance human-AI collaboration integrating deductive verification methods and insights from historical high-quality schemes. The typical pattern hidden in historical high-quality schemes, such as change of task priorities in shared resources, provides critical guidance for intelligent agents in learning and decision-making. By utilizing deductive verification methods, we proposed pattern-driven correctness learning (PDCL), formally modeling and reasoning the adaptive behaviors—or “correctness pattern”—of system agents based on historical high-quality schemes, capturing the logical relationships embedded within these schemes. Using this logical information as guidance, we establish a correctness judgment and feedback mechanism to steer the intelligent decision model toward the “correctness pattern” reflected in historical high-quality schemes. Extensive experiments across multiple working conditions and core parameters validate the framework’s components and demonstrate its effectiveness in improving decision-making and resource optimization.

1 Introduction

With the growing adoption of intelligent decision-making support systems (IDSS) in safety-critical domains such as smart manufacturing ([Li *et al.*, 2022]), transportation ([Visan *et al.*, 2022]), and electricity management ([Mansouri *et al.*, 2023]), the demand for enhanced system correctness, reliability and trustworthiness has increased.

The correctness of IDSS generally refers to its ability to produce accurate outputs for valid inputs. “Correctness” is defined relative to human judgment ([Sokol and Vogt, 2024]), assuming that humans can make correct judgments. Thus,

an IDSS is considered correct if and only if, for any input, the judgments made by humans and the system are identical. Reinforcement learning from human feedback (RLHF) guides the agents to converge in the right direction by providing interactive feedback to the decision model [Kaufmann *et al.*, 2023]. However, human evaluation on decision-making outcomes in complex logical tasks is often imprecise, limited by individual experience, preferences, and intuition. These limitations pose significant challenges for effectively training decision models.

Formal verification constitutes a rigorous mathematics-based technology for the specification, verification, and design of computation systems, serving as a crucial approach to enhance and ensure the correctness of these systems. Formal verification techniques are primarily categorized, according to methodological classifications, into deductive verification, model checking, and abstract interpretation. Integrating formal verification into IDSS has emerged as a significant research focus ([Verma *et al.*, 2019; Beard and Baheri, 2022; Hunt *et al.*, 2021; Kouvaros, 2023; Ghosh, 2023]). Recent efforts have explored verifying intelligent decision-making algorithms using formal verification techniques such as model checking ([Krichen *et al.*, 2022; Fu *et al.*, 2018]) and abstract interpretation ([Landers and Doryab, 2023; Albarghouthi *et al.*, 2021]). However, these studies have yet to fully address the verifiability challenges posed by IDSS in decision-making contexts, including the need for more complete correctness proofs of decision output schemes, the implementation of compositional reasoning for intelligent decision-making, and the development of a formal-specification-driven design framework.

As another formal verification technique, deductive verification employs formal languages, semantics, logical reasoning, and theorem proving tool to ensure the correctness of computation systems. Beyond verification, this technique facilitates a deep understanding of the system behavior [Wolfman and Weld, 1999], which in turn aids in guiding the design of the system. Adapting and applying the deductive reasoning techniques to the field of intelligent decision-making is an alternative way to deal with the problems mentioned above. However, formal verification approaches based on deductive reasoning remain relatively underexplored in IDSS. This limitation arises because deductive verification requires a formal

*Corresponding authors

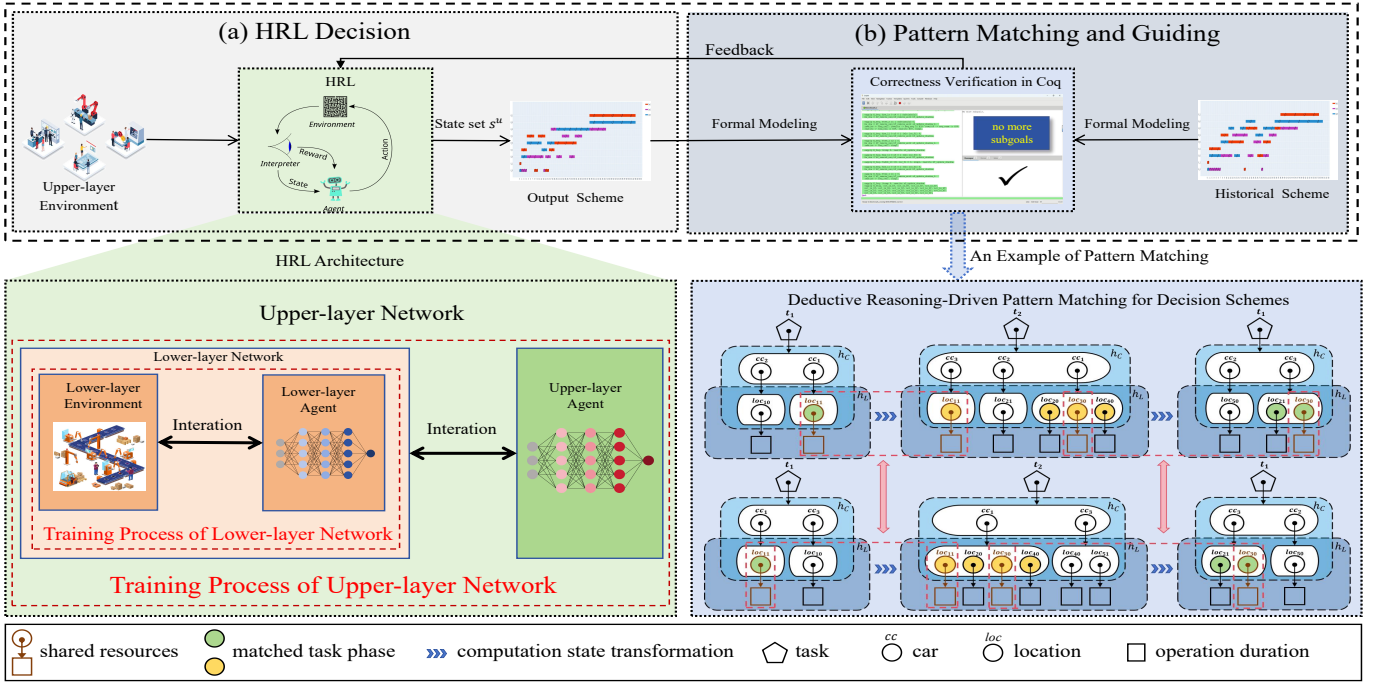


Figure 1: Overview of the proposed correctness learning framework PDCL. In the first stage, a hierarchical reinforcement learning (HRL) model is constructed to generate output schemes. In the second stage, typical correctness patterns (task priorities) of historical high-quality schemes and output schemes are formally proved in Coq and feedback is given to the model based on the degree of pattern matching.

definition of correctness and a clear understanding of the principles underlying the target system’s operation, both of which remain unresolved in this field.

To bridge this gap, we focus on ensuring the correctness of output instructions generated by IDSS while providing precise descriptions and specifications of the behavior of agents, rather than formalizing the inherently complex decision-making process. By doing so, we introduce deductive verification into intelligent decision-making models for the first time, and propose correctness learning (CL) with the following core concept: verifying the correctness of the decision output instructions (i.e., decision schemes). Simultaneously, it deduces, specifies, and symbolically describes the hidden and cumulative behavior of agents from the execution process of the instructions, and then sets a benchmark with respect to the formalized agents’ behavior to guide the evolution of the learning model along with the expected direction.

In sight of the above, we propose a pattern-driven correctness learning (PDCL): taking historical high-quality schemes as the benchmark for correctness, by identifying the behavioral patterns in historical high-quality schemes, the “correctness pattern” in historical schemes is injected into the decision-making model to improve performance. Specifically, first, we decouple the process decision from resource allocation, executing them separately at the upper and the lower layers. At the lower layer, we train a resource allocation network, which, upon convergence, is integrated into the upper-layer environment to provide real-time feedback for the process decision network. Simultaneously, the process decision network is trained to handle scheduling processes,

ultimately generating complete scheduling schemes. Second, we conduct deductive verification of historical high-quality schemes utilizing the mathematical reasoning capabilities of separation logic for shared resource allocation and management. By modeling, analyzing, and reasoning the scheme execution, we symbolically describe the typical “pattern” such as local resource utilization, allocation and release, resource occupation, and task prioritization. Third, deductive verification ensures the correctness of decision output schemes of the decision model and evaluates the extent to which the intermediate output schemes of the decision model exhibiting the typical pattern match historical high-quality schemes. A reward mechanism, based on the principle that a higher matching degree with these patterns yields higher rewards, incentivizes the model to adjust toward the desired direction. This approach enables the model to surpass traditional scheduling methods, achieving more efficient resource allocation.

Overall, the contributions of this paper are as follows:

- We are the first to introduce deductive verification into IDSS, and propose correctness learning, accomplishing the verification of decision schemes and the symbolic description of the behavior of agents, by which establishing a novel learning mechanism.
- We propose a pattern-driven correctness learning, which effectively combines the insights derived from historical high-quality experiences with the robust exploratory capabilities of intelligent learning algorithms.
- We extensively evaluate PDCL across different working conditions, the performance of the four benchmark al-

gorithms improved by an average of 8.4%, 3.9%, 1.6%, and 5.7%, respectively, and we also analyze the impact of core parameters on the effectiveness of PDCL.

2 Related Work

2.1 Reinforcement Learning for Human Feedback

[Christiano *et al.*, 2017] introduced human experience to assist model learning in deep reinforcement learning. Subsequently, several scholars studied the intricate interaction between human experience and intelligent agents [Kaufmann *et al.*, 2023; Chakraborty *et al.*, 2024; Zhang *et al.*, 2024; Crochepierre *et al.*, 2022]. We focus on the sources of feedback information for intelligent agents, including large language models (LLMs), human experience, and logical reasoning. [Brooks *et al.*, 2023] implemented policy iteration using a contextual learning mechanism over an LLM, enabling it to perform reinforcement learning tasks without expert demonstrations or gradients. [Cao *et al.*, 2024] leveraged logical rules derived from the environment to decompose task goals and guide agents to enhance human-AI perception and collaboration. Compared to the above methods, we alleviate the inherent limitations of current machine learning methods in terms of explainability by embedding verification based on deductive reasoning into the learning process.

2.2 Safe Reinforcement Learning

Safety reinforcement learning is divided into constrained reinforcement learning [Bai *et al.*, 2023; Bharadhwaj *et al.*, 2020], shielded reinforcement learning [Carr *et al.*, 2023; Beard and Baheri, 2022; Odriozola-Olalde *et al.*, 2023] and risk-constrained policy gradients [Xiao *et al.*, 2024]. Shielded reinforcement learning combines formal verification with reinforcement learning and introduces “shielding” to verify whether the agent’s behavior is safe and check shield dangerous behaviors. The above work only focused on process reliability, limiting the decision path to a range of satisfying properties, and did not consider using theorem-proving methods to embed the correctness of decision results to help improve decision-making effects.

3 Problem Formulation

In this section, we formally define scenario modeling and introduce it in detail.

Definition 1 (Operation). An operation is a two-entry tuple $o = (w, t)$, where w represents the resources required by the operation and t represents the execution duration of the operation.

Definition 2 (Task). A task is a two-entry tuple $\tau = (O, \beta)$, where O is a set representing the operations required to complete a task, and the set of operations contained in a task must be executed sequentially. β represents the progress of task completion.

Definition 3 (Equipment). An equipment can be represented as a two-entry tuple $e = (w, n)$, where w represents the type of resources that the equipment can provide and n represents the number of workstations that the equipment can provide.

Definition 4 (Car). A car is a two-entry tuple $c = (l, b)$, where l represents the location and b represents whether it is available.

Definition 5 (Job). Given a set of tasks Γ associated with a set of O , a set of C and a set of equipment E , job scheduling assigns appropriate devices $e \in E$ to perform a job based on the resources required by operation $o \in O$ of task $\tau \in \Gamma$. Its goal, T^g is to minimize the total completion time of each batch of tasks, which can be defined as

$$T^g = \min \sum_{\tau \in \Gamma} \sum_{o \in O} \sum_{e \in E} T^e(\tau, o) + T^w(\tau, e \vee c) \quad (1)$$

where T^e represents the time required for the task to execute the job, and T^w represents the time the task waits for the allocation of equipment or car.

4 Algorithm

In this section, we describe the construction of hierarchical reinforcement learning, deductive verification, and model training in detail. The overview is shown in Figure 1.

4.1 Hierarchical Reinforcement Learning

Lower-layer Model

States s^l : The state space of the lower-layer model at time t is defined as: $s^l = (\tau_t, E_t^l, C_t^l)$, where τ_t represents the state matrix of one task, E_t^l represents the state matrix of the equipments, C_t^l is the state matrix of the cars. The initial state of the car is randomly generated.

Actions a^l : The lower-layer model selects the most suitable car from multiple available cars to complete the task. The action space is defined as $a_t^l \in \{0, 1, 2, \dots, i, \dots, K\}$. The action $a_t^l = 0$ indicates to keep waiting and not select a car, $a_t^l = i$ indicates the specific serial number of selected cars, and K is the total number of cars.

Reward function r^l : The lower-layer model reward function consists of the task reward r_x^l and the process reward r_y^l , expressed as $r^l = r_p + r_q$, where r_p is the task reward \mathcal{R} obtained when the task reaches the target location, and \mathcal{R} is a constant. r_q is the immediate feedback during the task and is defined as

$$r_q = \begin{cases} 2, & \exists C_{d,t}^l = 1 \wedge a_t^l = d \\ 1, & \forall C_t^l = -1 \wedge a_t^l = 0 \\ -2, & \exists C_t^l = 1 \wedge a_t^l = 0 \\ -2, & \forall C_t^l = -1 \wedge a_t^l \neq 0 \\ -2, & \exists C_t^l = 1 \wedge C_{d,t}^l = -1 \wedge a_t^l = d \end{cases} \quad (2)$$

1) If both the equipment and car are idle and an action is assigned to the agent, a reward is given. 2) If there is no idle time for the equipment or car when the agent chooses to wait, a rewarded is given. 3) If the agent chooses to allocate when there is no idle time on the equipment or car, a penalty is imposed. 4) If there is no idle time for equipment and cars, but actions are assigned to the agent, a penalty is imposed. 5) If the cars are idle, a non-idle car is assigned to the agent, and a penalty is imposed.

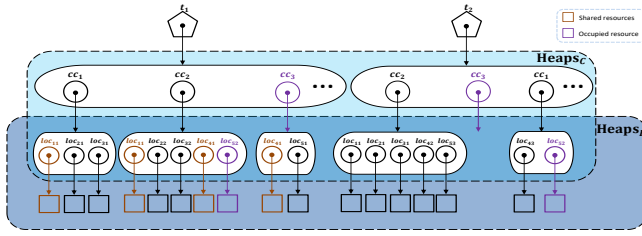


Figure 2: Schematic diagram of the two-tier resource heap model of the job scheduling system.

Upper-layer Model

States s^u : The state space of the upper-layer model at time t is defined as: $s^u = (\Gamma_t, E_t^u, C_t^u, F_t)$, where Γ_t represents the state matrix of tasks, E_t^u represents the state matrix of the equipment, C_t^u is the state matrix of the car, and F_t is used to describe the completion progress of job scheduling.

Actions a^u : The action space contains the set of task scheduling decisions that can be executed in different states. It is defined as $a^u \in \{1, \dots, i, \dots, N\}$. Among them, $a_t^u = i$ means that the i -th task selected in a given state is assigned to the equipment.

Reward function r^u : r^u : The upper-layer model focuses on the overall task completion, and the reward value is defined as $r_t^u = r_x + r_y + r_z$. r_x is determined by the maximum time spent on each decision-making process. The smaller the time difference between two consecutive decisions, the higher the parallelism of the two tasks on the timeline. This reward mechanism encourages the agent to increase task parallelism to improve overall task efficiency. r_x is defined as:

$$r_x = \frac{M^{old} - M^{new}}{5000} \quad (3)$$

M represents the maximum value of the overall time step of the system after the execution of the job scheduling mission. This parameter reflects the maximum time required at the beginning of the mission.

r_y is used to constrain the decision-making behavior and impose penalties when the task reaches the target location and is still selected. It is defined as:

$$r_y = -1 - \frac{(\mathcal{N} - F_t)}{\mathcal{N}} \quad (4)$$

\mathcal{N} is a constant used to represent the completion progress of job scheduling.

After each round of training, if the scheme obtained can complete all tasks, we will verify the current scheme. By comparing the output scheme with the historical high-quality scheme, get r_z according to the matching degree, defined as:

$$r_z = -\alpha * (\mu_{match} - \mu_{total}/2) \quad (5)$$

where μ_{match} represents the matching degree between the pattern obtained in the output scheme and the historical high-quality scheme, and α is the weight coefficient.

4.2 Deductive Verification

Formal model of the job scheduling system

Based on separation logic, the behavior of the job scheduling system is formally modeled as a two-layer, resource-

separated, two-tier heap structure model, as shown in Figure 2. The core components of this model are the ‘‘car resource heap’’ (i.e., $Heaps_C$ in the Figure 2) and the ‘‘location resource heap’’ (i.e., $Heaps_L$ in the Figure 2, the location of the equipment). The car resource heap establishes a relationship between the ‘‘mapping from task to car’’ and the ‘‘mapping from the car to location’’ while ensuring the mutual independence of the car resources. Conversely, the location resource heap is used to describe the underlying operation mode of the transport task, in which each location represents a shared deployable resource. By doing so, this model possesses sufficient expressive power to describe the behavior of the job scheduling system, encompassing 1) the interrelationship between the two types of resources, 2) the sequence of workflow execution process established within the scheme, 3) cooperative scheduling among multiple tasks, and 4) the prolongation of resource occupancy resulting from extensive resource sharing.

1 Function benchmark()	8 ...	15 ...	22 ...
2 ...	9 $c_1^a := \text{plan}(n_1);$	16 $j := \#t_2, l;$	23 $c_1^a := \text{plan}(n_2);$
3 $c_1^a := \text{plan}(n_1);$	10 $\text{att}(t_i, c_1^a);$	17 while $1 \leq j$ do	24 $\text{att}(t_i, c_1^a);$
4 $t_i := \text{asgn}(c_1^a);$	11 lstexe $t_i, l;$	18 lstexe $t_i, l;$	25 ...
5 ...	12 ...	19 $j := j - 1;$	26 end
6 lstexe $t_i, l;$	13 $c_1^a := \text{plan}(n_2, n_3, n_4);$	20 end while	
7 free $t_i, l;$	14 $\text{att}(t_i, c_1^a);$	21 free $t_i, l;$	

Figure 3: Modeling program of the historical high-quality schemes (simplified)

Modeling language of the job scheduling system

Based on the aforementioned two-tier resource heap model, a modeling language for the job scheduling system called ML_{JSS} is constructed. It primarily describes the resource allocation and management operations during the actual execution of the operation scheme. In the following, the syntax of the modeling language is defined, along with its computational state and operational semantics.

Definition 6. The full syntax of the expressions and commands of ML_{JSS} is given as follows:

$$\begin{aligned}
 e &:= n, m, \dots \mid x, y, \dots \mid e_1 + e_2 \mid e_1 - e_2 \mid e_1 \times e_2 \mid \#ce \mid \#t \\
 be &:= e_1 = e_2 \mid e_1 \leq e_2 \mid \text{true} \mid \text{false} \mid \neg be \mid be_1 \vee be_2 \mid be_1 \wedge be_2 \\
 te &:= \text{null} \mid \text{fin} \mid t_1, t_2, \dots \mid te \cdot ce \mid te_1 \cdot te_2 \\
 ce &:= \text{null} \mid n, m, \dots \mid c_1^a, c_2^a, \dots \mid t.e \\
 C &:= x := e \mid C; C' \mid \text{if } be \text{ then } C \text{ else } C' \mid \text{while } be \text{ do } C' \\
 &\quad \mid t := \text{asgn}(ce^*) \mid \text{att}(t, ce^*) \mid \text{free } t.e \mid \text{comp } t \\
 &\quad \mid c^a := \text{plan}(\bar{e}) \mid \text{add}(c^a, e) \mid x := \{ce.e\} \mid \text{lstexe } t.e
 \end{aligned} \quad (6)$$

where e is written for location expressions, be for Boolean expressions, te for task expressions, ce for car expressions, and C for commands (including the standard IMP command inherited in the first line and the newly added task and car operation commands in the last two lines).

The computational state of the modeling language ML_{JSS} is defined as a quintuple, i.e., a state $\sigma \in \text{States}$ is of the form $(s_T, s_C, s_L, h_C, h_L) \in \text{Stores}_T \times \text{Stores}_C \times \text{Stores}_L \times \text{Heaps}_C \times \text{Heaps}_L$.

Algorithm 1 Hierarchical reinforcement learning decision model training

Input: The maximum number of training steps T , trained lower-layer policy network π_{θ_l} , upper-layer policy network π_{θ_u} reward coefficient α , query function fun , verification tools Coq, the historical high-quality scheme h , constant \mathcal{N} .

Output: tuple $(s_t^u, a_t^u, r_t^u, s_{t+1}^u)$.

- 1: **while** T **do**
 - 2: The upper-layer policy network π_{θ_u} selects an action a_t^u based on the state s_t^u .
 - 3: Obtain the lower-layer state s_t^l based on the upper-level action a_t^u and the current state s_t^u .
 - 4: Use the trained lower-layer policy network π_{θ_l} to directly generate the action a_t^l .
 - 5: Execute the lower-layer action a_t^l and obtain the next state s_{t+1}^l from the lower-layer environment.
 - 6: Update the upper-layer state to get s_{t+1}^u based on the lower-layer state s_{t+1}^l .
 - 7: Get rewards $r_t^u = r_x + r_y$
 - 8: **if** $F_t = \mathcal{N}$ **then**
 - 9: $r_t^u = \alpha * fun(Coq(s_t^u), Coq(h)) + r_t^u$
 - 10: **end if**
 - 11: **end while**
 - 12: **return** experience tuple $(s_t^u, a_t^u, r_t^u, s_{t+1}^u)$
-

Definition 7. The operational semantics for the plan command of ML_{JSS} is given below as an example. The complete semantics is given in Appendix B.

$$\frac{cc \in \mathcal{C} - \text{dom}(h_C) \text{ and } loc_1, \dots, loc_n \in \text{Loc} - \text{dom}(h_L)}{\langle c^a := \text{plan}(\bar{e}), \sigma \rangle \rightsquigarrow (s_T, [s_C | c^a : cc], s_L, [h_C | cc : (loc_1, \dots, loc_n)], [h_L | loc_1 : [[e_1]]\sigma, \dots, loc_n : [[e_n]]\sigma])} \quad (7)$$

Intuitively, this command plans the process undertaken by car c ; that is, it assigns a location sequence to the car based on the order of the workflow, and the corresponding operation duration value of each location constitutes sequence \bar{e} .

Correctness verification of the schemes

The correctness of a scheme can be ensured by describing the scheme as a modeling program by ML_{JSS} and checking whether the execution behavior of this program is as expected according to the operational semantics of ML_{JSS} . We subsequently demonstrate our verification method by proving the sample modeling program in Figure3, which describes the dynamic implementation process of the historical high-quality schemes. The sample program involves the allocation and management of two types of resources, cars, and locations, also known as the resource consumption reference in the real-world engineering field. To enhance readability, we isolate two of the shared resource sub-tasks in the scheme for demonstration. This is feasible because of the local reasoning strategy in separation logic, permitting our reasoning locally to focus only on the sub-resource heap that is mutated and ignore all others.

Proof sketch. Starting from a given initial state $(s_T, s_C, s_L, h_C, h_L)$ (Line 2), according to the order of the workflow in

the scheme, a car c_1^0 is planned to perform an operation of the first phase of one task at an implicit location loc_{11} with operation duration n_1 (Line 3), and a task t_0 is subsequently assigned to this car (Line 4). By the operational semantics of the **plan** and **asgn** commands, the initial state is transitioned to $([s_T | t_0 : cc_1], [s_C | c_1^0 : cc_1], s_L, [h_C | cc_1 : (loc_{11})], [h_L | loc_{11} : n_1])$. We then execute the first item of the sequence of operations associated with task t_0 , that is, removing the first item of the location sequence corresponding to the car resource cc_1 in h_C and releasing the corresponding location resource loc_{11} from h_L (Line 6). Subsequently, we release the car resource cc_1 , whose content value is required to be an empty sequence **null**, corresponding to the first operation of task t_0 from h_C , that is, c_1^0 . The state is now $([s_T | t_0 : \text{null}], [s_C | c_1^0 : cc_1], s_L, h_C, h_L)$. In Line 9, a new car c_3^8 is planned for an operation of the first phase of one task at the same location loc_{11} of the first operation of task t_0 , which is previously released in the previous step, and then attach this car to the end of an existing task t_8 (Line 10), thus obtaining a state $([s_T | t_8 : cc_3], [s_C | c_3^8 : cc_3], s_L, [h_C | cc_3 : (loc_{11})], [h_L | loc_{11} : n_1])$. The first operation of task t_8 is then executed in Line 11 in a similar manner to Line 6, resulting in a state $([s_T | t_8 : cc_3], [s_C | c_3^8 : cc_3], s_L, [h_C | cc_3 : \text{null}], h_L)$. Subsequently, in Line 13, the released car cc_1 is activated again and is planned to undertake three consecutive phases of the task t_8 , allocating three new location resource loc_{20} , loc_{30} and loc_{40} , and their corresponding operation duration form a sequence (n_1, n_2, n_3) . After attaching this car to task t_8 in Line 14, state $([s_T | t_8 : cc_1], [s_C | c_1^8 : cc_1], s_L, [h_C | cc_1 : (loc_{20}, loc_{30}, loc_{40})], [h_L | loc_{40} : n_4 | loc_{30} : n_3 | loc_{20} : n_2])$ is obtained. Through the command between Line 16 and Line 20, involving a while loop, the three phases of the task t_8 are executed successively. After removing the corresponding car resource c_1^8 from task t_8 in Line 21, state $([s_T | t_8 : \text{null}], [s_C | c_1^8 : cc_3], s_L, h_C, h_L)$ is obtained. Subsequently, the second phase of the task t_0 is deployed in Line 23-24, resulting in a state $([s_T | t_0 : cc_3], [s_C | c_3^0 : cc_3], s_L, [h_C | cc_3 : (loc_{20})], [h_L | loc_{20} : n_2])$. The remainder describes the subsequent implementation of the scheme; therefore, it is not repeated.

In contrast to task t_8 , which can be assigned and executed continuously in Lines 9-21, task t_0 was divided into two task phases. Thus, the first and second stages start at Lines 3 and 23, respectively, to meet the established process timing of the scheme. The transformation relation between configurations shows that the two task-running processes share two locations, namely, loc_{11} and loc_{20} , and meet the established requirements of the scheme. Thus, the t_0 task at loc_{11} has a higher sequential priority, whereas the t_8 task at loc_{20} has a higher sequential priority. In the above verification process, we identified and symbolically represented the hidden phenomenon of the stable operation of the job scheduling system, such as the law of change in the priority of workflow under resource preemption.

Formal Development in Coq

Based on the above formalization, we implemented the modeling language ML_{ASS} in proof assistant Coq, in which we interactively verified the correctness of the historical high-quality schemes(as described in Figure3) and the intelligent

Table 1: Test results of different algorithms and different algorithms with rule-guided strategies across ten task scenarios and twelve task scenarios. Four indicators are used for evaluation: completion time (ComT, lower the better), cumulative reward (CumR, higher the better), decision time (DecT, higher the better), and training time (TraT).

Method	Ten Tasks				Twelve Tasks			
	ComT ↓	CumR ↑	DecT ↓	TraT	ComT ↓	CumR ↑	DecT ↓	TraT
DQN	64	-0.0128	52.37	430	68	-0.0136	59.97	524
DDQN	60	-0.0120	20.41	355	71	-0.0142	46.05	1026
Dueling DQN	58	-0.0116	22.47	354	68	-0.0136	24.39	313
PPO	63	-0.0126	79.72	324	80	-0.0160	80.97	417
DQN & PDCL	58	-0.0116	53.46	496	63	-0.0126	64.24	930
DDQN & PDCL	57	-0.0114	21.70	359	69	-0.0138	56.92	1204
Dueling DQN & PDCL	57	-0.0114	24.12	371	67	-0.0134	25.71	412
PPO & PDCL	59	-0.0118	80.91	425	76	-0.0152	83.10	561

Table 2: The test results of different algorithms and different algorithms with rule-guided strategies across ten task scenarios after adjusting the learning rate.

Method	ComT ↓	CumR ↑	DecT ↑	TraT
DQN	57	-0.0114	67.13	372
DDQN	56	-0.0112	40.07	890
Dueling DQN	56	-0.0112	66.17	438
PPO	75	-0.0150	75.33	607
DQN & PDCL	56	-0.0112	69.24	382
DDQN & PDCL	56	-0.0112	45.05	1081
Dueling DQN & PDCL	56	-0.0112	67.64	971
PPO & PDCL	74	-0.0148	77.77	649

decision model output scheme, and symbolically analyzed the pattern contained in the scheme. The development is available online at the following URL. A diagram of the Coq deployment is given in Appendix C.

With this tool, one can write the scheme to be verified into a modeling program and interactively prove the termination and execution correctness of this modeling program to ensure the correctness of the scheme. Moreover, during verification, the transformation relationship between the configurations of the execution process of operation commands can be analyzed based on the operational semantics of the corresponding commands. This symbolically describes the hidden and cumulative adaptive behavior properties and pattern of the subject within the operating system.

4.3 Model Training

As shown in Algorithm 1, the upper-layer model is trained to ensure the processing of a single task. At this stage, the low-layer model focuses on the car’s allocation. Subsequently, the upper-layer module obtains state s_t^l based on state s_t^u and action s_{t+1}^u . The action is generated using the trained low-layer model; the bottom-level action is executed; the next state s_{t+1}^l is obtained from the execution model environment; and the top-level state is updated with state s_{t+1}^l to obtain S_{t+1}^l and the reward value r_t^u . To better conduct interactive training, we abstract the resource priority transforma-

Table 3: The test results of different algorithms and different algorithms with rule-guided strategies across ten task scenarios after adjusting the activation function.

Method	ComT ↓	CumR ↑	DecT ↑	TraT
DQN	57	-0.0114	50.98	799
DDQN	-	-1.0453	50.46	475
Dueling DQN	-	-1.1588	52.94	423
PPO	61	-0.0122	78.93	226
DQN & PDCL	56	-0.0112	59.82	856
DDQN & PDCL	-	-1.0616	53.49	627
Dueling DQN & PDCL	56	-0.0112	66.57	648
PPO & PDCL	59	-0.0118	80.75	227

tion phenomenon found in the deductive reasoning process into rules to verify the degree of pattern matching between the output plan and the historical high-quality plan. The design of the reward mechanism follows the principle that the more rules are matched, the greater the reward value, so that the model breaks through the original scheduling plan and achieves more efficient resource allocation.

5 Experimental Evaluation

5.1 Experimental Setting

Simulation environment. Simulation environment reference [Yujie *et al.*, 2023] construction. In the simulation scenario, each task consists of five operations that must be executed in sequence. Equipment is divided into five categories, each supporting different operations, and each piece of equipment has a different number of workstations. Cars provide general resources. Different operations require a car and corresponding equipment to be performed. We do not consider the car’s transit time. The car and equipment can only be obtained by one operation at a time and released after completion. The experiment built two simulation scenarios for evaluation. The first scenario includes ten tasks, three cars, and the number of workstations in the five pieces of equipment were two, two, two, one, and two. The second scenario included 12 tasks, and the number of workstations in the five pieces of equipment was the same as that in the first scenario. Machine learn-

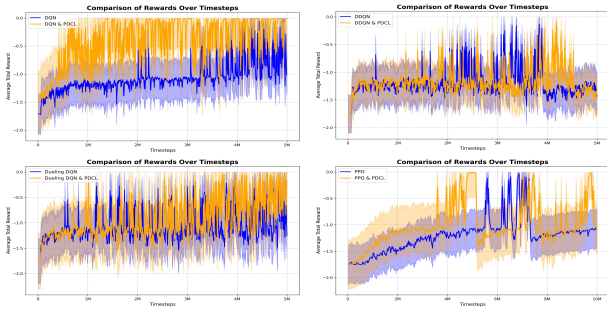


Figure 4: Results of different algorithms and joint pattern guidance on 10 tasks.

ing methods are trained with Intel i9-14900K CPU, GTX4090 GPU a, 64GB RAM or Intel i7-13900K CPU, GTX4080 GPU a, 32GB RAM. The same algorithm was tested on the same computer to ensure the readiness of the verification results.

Evaluation metrics. Completion time (ComT), cumulative reward (CumR), decision time (DecT), and training time (TraT) were used as metrics to measure the performance of the above methods, where ComT is the time slice length of the above methods, where ComT is the time slice length of the above methods, where ComT is the time slice length of the above methods, where ComT is the time slice length of the above methods. CumR is the total value of the rewards accumulated in one period. DecT is the total time required to assign a specified number of tasks using the trained model in milliseconds. TraT is the total time spent training for one period in minutes.

Compared approaches. The algorithms we use are implemented from [Raffin *et al.*, 2021]. The lower-layer model training uniformly uses PPO, whereas the upper-layer model uses DQN, PPO, DDQN, and Dueling DQN. We then added pattern matching to the environment to guide retraining of the decision model. During training, all the models maintained fixed hyperparameters relative to themselves. PPO was trained for 10 million steps, with Tanh as the activation function, while DQN, DDQN, and Dueling DQN were trained for 5 million steps, with Sigmoid as the activation function. Except for Dueling DQN with a learning rate of $2e-5$ in the 12-task scenario, the learning rate of other scenarios was uniformly set to $2e-4$.

5.2 Result Analysis

Simulation environment 1. Table 1 lists the performance of the different algorithms and the addition of rpattern guidance in simulation environment 1. From the perspective of the cumulative completion time, after adding pattern guidance, the effects of DQN, DDQN, Dueling DQN, and PPO were improved by 9.4%, 3.4%, 1.8%, and 6.4%, respectively. Regarding training time, the time of each algorithm increased significantly compared with that without pattern guidance because the agent can conduct more exploration in each epoch under pattern guidance (Figure 4). After adding pattern guidance during the training process, the average cumulative reward per round was much higher than that without adding pattern guidance. Simultaneously, regarding response time, after adding pattern guidance, it increased by 1.09 ms, 1.39 ms, 1.65 ms, and 1.1 ms, respectively, which did not affect the real-time performance of the algorithm. To improve perfor-

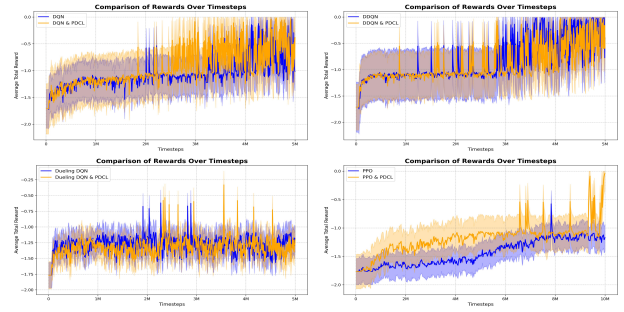


Figure 5: Results of different algorithms and joint pattern guidance on 12 tasks.

mance, only a minimal compromise in real time was required.

Simulation environment 2. To further explore the effects of different operating conditions on CFL, we conducted a set of experiments by increasing the operating conditions from 10 to 12. As shown in Table 1, the completion times of DQN, DDQN, Dueling DQN, and PPO were reduced by 5 min, 2 min, 3.4 min, and 4 min, respectively. As shown in Figure 5, after adding pattern guidance, the number of scheduling tasks completed by each algorithm was significantly improved compared with the number without pattern guidance.

Additional experiment1. We set the learning rate to $2e-5$. As shown in Table 2, after adding pattern guidance, the scheduling times of Dueling DQN and PPO reduced by 1 and 2 min, respectively, which proves that our framework remains effective after adjusting the learning rate. Although the effects of DQN and DDQN did not improve, we found that this was close to the optimal solution. However, the Appendix A shows that the speed and training stability significantly improved after adding pattern guidance.

Additional experiment2. We set the activation function to ReLU, and PPO was trained to change to 5 million steps. As shown in Table 3, although the response and training times of each algorithm increased slightly after adding pattern guidance, the scheduling effect improved, which was acceptable. Notably, before adding pattern guidance, the Dueling DQN could not converge; however, after adding pattern guidance, it completed the scheduling task. Therefore, the model can better complete the scheduling task after learning the priority of the resource allocation. Simultaneously, after adjusting the hyperparameters, the pattern guidance remains effective.

6 Conclusion

We propose correctness learning incorporating deductive verification and historical high-quality schemes. Leveraging the reasoning capabilities of separation logic applied to shared resources, we model and reason the task priorities hidden in the scheme. The matching degree between the task priorities in the model output scheme and the task priorities in the high-quality scheme guides the training process, which effectively combines the historical experience with the exploratory capability of the reinforcement learning. The experimental results demonstrate that our method enables multiple algorithms to surpass their original performance in diverse conditions. In the future we will identify more general pattern by analyzing

more historical high-quality schemes. Additionally, we will investigate the different importance of different pattern within the overall decision-making framework.

References

- [Albarghouthi *et al.*, 2021] Aws Albarghouthi, Zidong Zhang, and Dongxia Zhang. Introduction to neural network verification. *Foundations and Trends® in Programming Languages*, 7(1–2):1–157, 2021.
- [Bai *et al.*, 2023] Qinbo Bai, Amrit Singh Bedi, and Vaneet Aggarwal. Achieving zero constraint violation for constrained reinforcement learning via conservative natural policy gradient primal-dual algorithm. In *Proceedings of the AAAI Conference on Artificial Intelligence*, volume 37, pages 6737–6744, 2023.
- [Beard and Baheri, 2022] Jared J Beard and Ali Baheri. Black-box safety validation of autonomous systems: A multi-fidelity reinforcement learning approach. *arXiv preprint arXiv:2203.03451*, 2022.
- [Bharadhwaj *et al.*, 2020] Homanga Bharadhwaj, Aviral Kumar, Nicholas Rhinehart, Sergey Levine, Florian Shkurti, and Animesh Garg. Conservative safety critics for exploration. *arXiv preprint arXiv:2010.14497*, 2020.
- [Brooks *et al.*, 2023] Ethan Brooks, Logan Walls, Richard L Lewis, and Satinder Singh. Large language models can implement policy iteration. *Advances in Neural Information Processing Systems*, 36:30349–30366, 2023.
- [Cao *et al.*, 2024] Chengzhi Cao, Yinghao Fu, Sheng Xu, Ruimao Zhang, and Shuang Li. Enhancing human-ai collaboration through logic-guided reasoning. In *The Twelfth International Conference on Learning Representations*, 2024.
- [Carr *et al.*, 2023] Steven Carr, Nils Jansen, Sebastian Junges, and Ufuk Topcu. Safe reinforcement learning via shielding under partial observability. In *Proceedings of the AAAI Conference on Artificial Intelligence*, volume 37, pages 14748–14756, 2023.
- [Chakraborty *et al.*, 2024] Souradip Chakraborty, Amrit Bedi, Alec Koppel, Huazheng Wang, Dinesh Manocha, Mengdi Wang, and Furong Huang. Parl: A unified framework for policy alignment in reinforcement learning from human feedback. In *The Twelfth International Conference on Learning Representations*, 2024.
- [Christiano *et al.*, 2017] Paul F Christiano, Jan Leike, Tom Brown, Miljan Martic, Shane Legg, and Dario Amodei. Deep reinforcement learning from human preferences. *Advances in neural information processing systems*, 30, 2017.
- [Crochepierre *et al.*, 2022] Laure Crochepierre, Lydia Boudjeloud-Assala, and Vincent Barbesant. Interactive reinforcement learning for symbolic regression from multi-format human-preference feedbacks. In *IJCAI*, pages 5900–5903, 2022.
- [Fu *et al.*, 2018] Chen Fu, Andrea Turrini, Xiaowei Huang, Lei Song, Yuan Feng, and Lijun Zhang. Model checking probabilistic epistemic logic for probabilistic multiagent systems. In *IJCAI International Joint Conference on Artificial Intelligence*, 2018.
- [Ghosh, 2023] Bishwamittra Ghosh. Interpretability and fairness in machine learning: A formal methods approach. In *IJCAI*, pages 7083–7084, 2023.
- [Hunt *et al.*, 2021] Nathan Hunt, Nathan Fulton, Sara Magliacane, Trong Nghia Hoang, Subhro Das, and Armando Solar-Lezama. Verifiably safe exploration for end-to-end reinforcement learning. In *Proceedings of the 24th International Conference on Hybrid Systems: Computation and Control*, pages 1–11, 2021.
- [Kaufmann *et al.*, 2023] Timo Kaufmann, Paul Weng, Viktor Bengs, and Eyke Hüllermeier. A survey of reinforcement learning from human feedback. *arXiv preprint arXiv:2312.14925*, 2023.
- [Kouvaros, 2023] Panagiotis Kouvaros. Towards formal verification of neuro-symbolic multi-agent systems. In *IJCAI*, pages 7014–7019, 2023.
- [Krichen *et al.*, 2022] Moez Krichen, Alaeddine Mihoub, Mohammed Y Alzahrani, Wilfried Yves Hamilton Adoni, and Tarik Nahhal. Are formal methods applicable to machine learning and artificial intelligence? In *2022 2nd International Conference of Smart Systems and Emerging Technologies (SMARTTECH)*, pages 48–53. IEEE, 2022.
- [Landers and Doryab, 2023] Matthew Landers and Afsaneh Doryab. Deep reinforcement learning verification: a survey. *ACM Computing Surveys*, 55(14s):1–31, 2023.
- [Li *et al.*, 2022] Chunquan Li, Yaqiong Chen, and Yuling Shang. A review of industrial big data for decision making in intelligent manufacturing. *Engineering Science and Technology, an International Journal*, 29:101021, 2022.
- [Mansouri *et al.*, 2023] Seyed Amir Mansouri, Ahmad Rezaee Jordehi, Mousa Marzband, Marcos Tostado-Véliz, Francisco Jurado, and José A Aguado. An iot-enabled hierarchical decentralized framework for multi-energy microgrids market management in the presence of smart prosumers using a deep learning-based forecaster. *Applied Energy*, 333:120560, 2023.
- [Odrozola-Olalde *et al.*, 2023] Haritz Odrozola-Olalde, Maider Zamalloa, and Nestor Arana-Arexolaleiba. Shielded reinforcement learning: A review of reactive methods for safe learning. In *2023 IEEE/SICE International Symposium on System Integration (SII)*, pages 1–8. IEEE, 2023.
- [Raffin *et al.*, 2021] Antonin Raffin, Ashley Hill, Adam Gleave, Anssi Kanervisto, Maximilian Ernestus, and Noah Dormann. Stable-baselines3: Reliable reinforcement learning implementations. *Journal of Machine Learning Research*, 22(268):1–8, 2021.
- [Sokol and Vogt, 2024] Kacper Sokol and Julia E Vogt. What does evaluation of explainable artificial intelligence actually tell us? a case for compositional and contextual validation of xai building blocks. In *Extended Abstracts of the CHI Conference on Human Factors in Computing Systems*, pages 1–8, 2024.

- [Verma *et al.*, 2019] Abhinav Verma, Hoang Le, Yisong Yue, and Swarat Chaudhuri. Imitation-projected programmatic reinforcement learning. *Advances in Neural Information Processing Systems*, 32, 2019.
- [Visan *et al.*, 2022] Maria Visan, Sorin Lenus Negrea, and Firicel Mone. Towards intelligent public transport systems in smart cities; collaborative decisions to be made. *Procedia Computer Science*, 199:1221–1228, 2022.
- [Wolfman and Weld, 1999] Steven A Wolfman and Daniel S Weld. The Ipsat engine & its application to resource planning. In *IJCAI*, volume 1999, pages 310–317. Citeseer, 1999.
- [Xiao *et al.*, 2024] Minheng Xiao, Xian Yu, and Lei Ying. Policy gradient methods for risk-sensitive distributional reinforcement learning with provable convergence. *arXiv preprint arXiv:2405.14749*, 2024.
- [Yujie *et al.*, 2023] LIU Yujie, HAN Wei, SU Xichao, and CUI Rongwei. Optimization of fixed aviation support resource station configuration for aircraft carrier based on aircraft dispatch mission scheduling. *Chinese Journal of Aeronautics*, 36(2):127–138, 2023.
- [Zhang *et al.*, 2024] Natalia Zhang, Xinqi Wang, Qiwen Cui, Runlong Zhou, Sham M Kakade, and Simon S Du. Multi-agent reinforcement learning from human feedback: Data coverage and algorithmic techniques. *arXiv preprint arXiv:2409.00717*, 2024.